

## Powder neutron diffraction of $\text{Tl}_2\text{BeF}_4$ at six temperatures from room temperature to 1.5 K

Iván da Silva,<sup>a\*</sup> Cristina González-Silgo,<sup>a</sup> Javier González-Platas,<sup>a</sup> Juan Rodríguez-Carvajal,<sup>b</sup> María Luisa Martínez-Sarrion<sup>c</sup> and Lourdes Mestres<sup>c</sup>

<sup>a</sup>Departamento de Física Fundamental II, Universidad de La Laguna, Avda.

Astrofísico Fco. Sánchez, s/n, E-38204 La Laguna, Tenerife, Islas Canarias, Spain,

<sup>b</sup>Laboratoire Léon Brillouin, CEA, Saclay, Grenoble, France, and <sup>c</sup>Departamento de Química Inorgánica, Universidad de Barcelona, Diagonal 647, E-08028 Barcelona, Spain

Correspondence e-mail: idasilva@ull.es

Received 7 July 2005

Accepted 11 October 2005

Online 11 November 2005

The structure of thallium fluoroberyllate,  $\text{Tl}_2\text{BeF}_4$ , has been analysed by the Rietveld method on neutron diffraction patterns collected at 1.5, 50, 100, 150, 200 and 300 K, with the aim of detecting low-temperature instabilities. Atomic parameters based on the isomorphous  $\beta\text{-K}_2\text{SO}_4$  crystal in the paraelectric phase were used as the starting model at room temperature; no evidence for any phase transition has been detected at lower temperature. The structure was determined in the orthorhombic space group  $Pnma$ . All the atoms (except one F atom) occupy sites with  $m$  symmetry. We have compared the structure with those of other compounds of the  $\beta\text{-K}_2\text{SO}_4$  family, at room temperature, in order to gain insight into their observed instabilities. The irregular coordination of the cations may indicate stereochemical activity of the  $\text{Tl}^{\text{I}}$  lone pair but does not indicate a possible structural instability.

### Comment

We are interested in the large family of ferroelectric compounds having the general formula  $A_2BX_4$  with the  $\beta\text{-K}_2\text{SO}_4$  structure in the paraelectric phase (space group  $Pnma$ ,  $Z = 4$ ). The most widely studied compounds are  $\text{K}_2\text{SeO}_4$ ,  $(\text{NH}_4)_2\text{SO}_4$  and  $(\text{NH}_4)_2\text{BeF}_4$ ; they exhibit interesting properties, related to a low-temperature phase transition which are strikingly different. For instance, the polar axis of  $(\text{NH}_4)_2\text{BeF}_4$  is the  $b$  axis, while that of both  $(\text{NH}_4)_2\text{SO}_4$  (Hoshino *et al.*, 1958) and  $\text{K}_2\text{SeO}_4$  is the  $c$  axis (Yamada *et al.*, 1984).  $(\text{NH}_4)_2\text{SO}_4$  has a ferroelectric phase transition at  $T_c = 223.5$  K (Schlemper & Hamilton, 1966), while an incommensurate phase is observed in  $(\text{NH}_4)_2\text{BeF}_4$  between  $T_i = 182.9$  K and  $T_c = 177.2$  K (Srivastava *et al.*, 1999), and in  $\text{K}_2\text{SeO}_4$  between  $T_i = 192.5$  K and  $T_c = 93$  K (Aiki & Hukuda, 1969). A review by Fábry & Pérez-Mato (1994) reported that the

instability of a large number of  $A_2BX_4$  compounds is related to the behaviour of the 11-coordinate cation rather than to the nine-coordinate cation, and especially to the bond strength of the shorter cation–anion contact parallel to the pseudo-hexagonal  $a$  axis. A detailed and comparative study of this type of compound is necessary. Alkali metal fluoroberyllates have been exceptional cases of  $A_2BX_4$ -type compounds in the past, and we have recently studied them by neutron powder diffraction with refinement in  $Pnma$  at room temperature and 1.5 K (da Silva *et al.*, 2005). Moreover, thallium oxysalts, such as  $\text{Tl}_2\text{SO}_4$ ,  $\text{Tl}_2\text{CrO}_4$  and  $\text{Tl}_2\text{SeO}_4$ , have also been studied; the last of these undergoes a phase transition at 72 K (Friese *et al.*, 2004). The different behaviour of thallium compounds with respect to other  $\beta\text{-K}_2\text{SO}_4$  compounds is a result of the

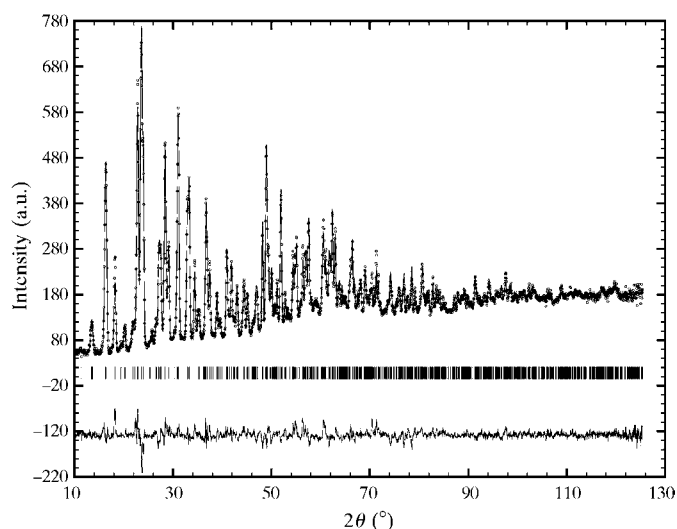


Figure 1

Plot of the Rietveld refinement result for  $\text{Tl}_2\text{BeF}_4$  at room temperature, showing the calculated (line), observed (circle) and difference (lower) profiles.

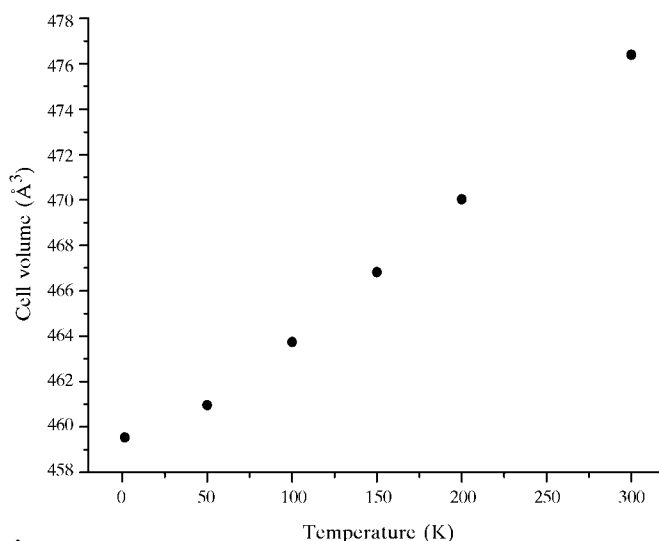


Figure 2

Variation of the unit-cell volume with temperature for  $\text{Tl}_2\text{BeF}_4$ , showing linear behaviour without anomalies.

stereoactivity of the  $6s^2$  lone pair in the  $Tl^I$  cation (Fábry & Breczewsky, 1993).

The aim of the present work is to compare the structure of  $Tl_2BeF_4$  with the rest of this class of compounds in order to assess the role of the cations in the structural instability. The correct crystal structure of  $Tl_2BeF_4$  has not been reported previously [only the cell parameters were reported by Arend *et al.* (1980)] and a structural phase transition has never been observed. We have measured the neutron powder diffraction patterns of  $Tl_2BeF_4$  at room temperature and lower temperatures down to 1.5 K, and we have refined the crystal structure using the Rietveld method in space group  $Pnma$  for all temperatures. The fitted diffraction profile at room temperature is shown in Fig. 1 and the variation of the unit-cell

volume with temperature is shown in Fig. 2. From DSC (differential scanning calorimetry) analysis and from Fig. 2, no thermal anomaly is observed. The structure of  $Tl_2BeF_4$  consists of isolated  $[BeF_4]^{2+}$  tetrahedra, with  $Tl^+$  ions distributed between them. The cations are placed in two different cavities; one cation, within a slightly distorted bipyramidal hole, remains 11-coordinate, while the other cation, within a distorted octahedral hole, is surrounded by nine F atoms. As in other fluoroberyllates (da Silva *et al.*, 2005) and thallium selenate (Friese *et al.*, 2004), the average Be–F bond length of the fluoroberyllate anion increases at low temperature (Table 1). At variance with other compounds showing structural instability (González-Silgo *et al.*, 1997; Solans *et al.*, 1998), (i) we do not observe any significant rotation of the tetrahedra around the  $b$  axis, so the environment of the cations is not changed with temperature, and (ii) the bond-valence sums (Brown, 1992) at both the Tl1 and the Tl2 sites are close to 1 v.u. for the entire temperature range. Otherwise, the five F atoms nearest to Tl1 are at distances less than 3.1 Å and lie on the same side of this cation (see Fig. 3a), thus indicating the stereoactivity of the Tl1 lone pair, as in other thallium compounds (Fábry & Breczewsky, 1993); this situation is maintained at lower temperatures. With respect to the Tl2 environment, the stereoactivity of the lone pair is less clear, although a tendency is observed at lower temperature; at 1.5 K, the three F atoms nearest this cation are at distances that are 0.1 Å shorter than the other Tl2–F contacts and lie approximately on the same side of Tl (Fig. 3b).

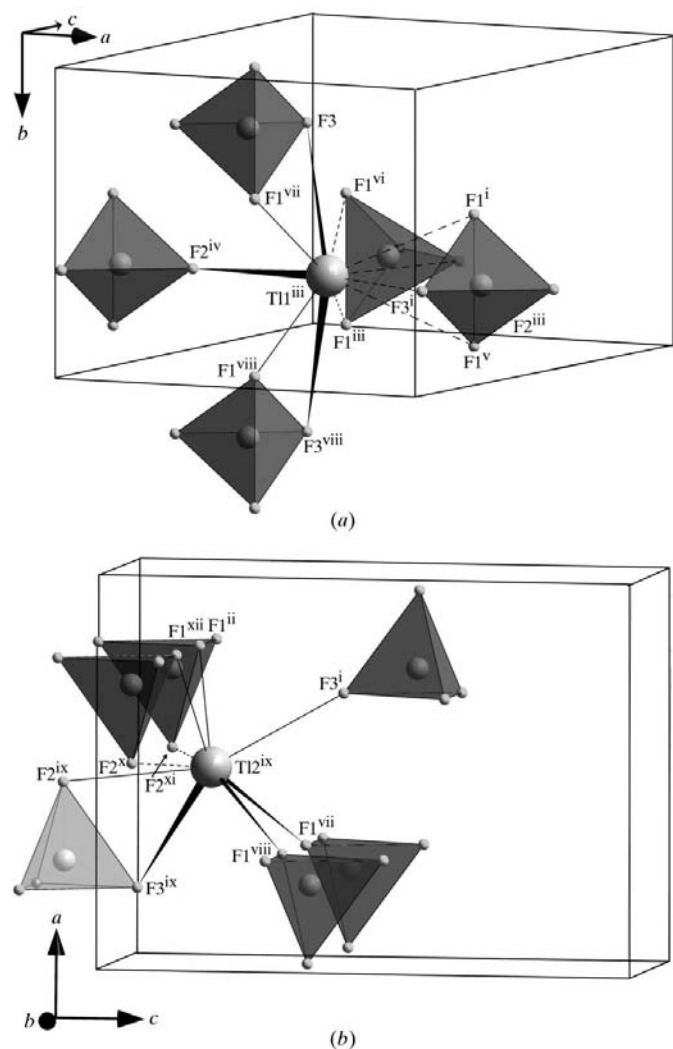


**Figure 3**  
Arrangement of the nearest-neighbour  $BeF_4$  tetrahedra to (a) 9- and (b) 11-coordinated  $Tl^+$  cations, showing the shortest (thick solid lines) and longest (thin dashed lines) bonds. Intermediate bonds are drawn with thin solid lines. [Symmetry codes: (i)  $1 - x, \frac{1}{2} + y, 1 - z$ ; (ii)  $\frac{1}{2} + x, \frac{1}{2} - y, \frac{1}{2} - z$ ; (iii)  $\frac{1}{2} - x, 1 - y, \frac{1}{2} + z$ ; (iv)  $-x, \frac{1}{2} + y, 1 - z$ ; (v)  $1 - x, 1 - y, 1 - z$ ; (vi)  $\frac{1}{2} - x, \frac{1}{2} + y, \frac{1}{2} + z$ ; (vii)  $x, \frac{1}{2} - y, z$ ; (viii)  $x, 1 + y, z$ ; (ix)  $\frac{1}{2} - x, 1 - y, -\frac{1}{2} + z$ ; (x)  $\frac{1}{2} + x, \frac{3}{2} - y, \frac{1}{2} - z$ ; (xi)  $\frac{1}{2} + x, \frac{1}{2} - y, \frac{1}{2} - z$ ; (xii)  $\frac{1}{2} + x, 1 + y, \frac{1}{2} - z$ .]

## Experimental

$Tl_2BeF_4$  was obtained *via* the reaction  $BeF_2(s) + H_2F_2(aq) + Tl_2CO_3(s) \rightarrow Tl_2BeF_4 + CO_2 + H_2O$ .  $BeF_2$ ,  $H_2F_2$  (48%) and  $Tl_2CO_3$  were of analytical grade. After completion of the reaction at pH 7, the sample was evaporated slowly at room temperature. After a few days, a polycrystalline powder was obtained. The sample was not evaporated to dryness so as to avoid possible contamination. The polycrystalline powder was filtered off and dried. Thermal analyses were carried out on a Perkin–Elmer differential scanning calorimeter Pyris I-DSC. The sample was measured in the temperature range 98–293 K, with a warming rate of 10 K  $min^{-1}$  and a total scale sensitivity of 0.1 mW. The sample mass was 27.76 mg. This analysis showed no thermal anomaly. A helium cryostat was used in order to keep the sample at the correct temperature during the diffraction experiments. We present the data collected at 1.5, 50, 100, 150, 200 and 300 K.

## $Tl_2BeF_4$ , all temperatures

### Crystal data

$Tl_2BeF_4$   
 $M_r = 493.77$   
Orthorhombic,  $Pnma$   
 $Z = 4$

Neutron radiation  
Specimen shape: cylinder  
50 × 10 × 10 mm  
White

### Data collection

Orphée reactor (Saclay, France) 3T2  
line diffractometer  
Specimen mounting: vanadium can

Specimen mounted in transmission  
mode  
Scan method: step  
Increment in  $2\theta = 0.1^\circ$

## Refinement

Refinement on  $I_{\text{net}}$   
Wavelength of incident radiation:  
1.2251 Å  
Excluded region(s): 0 to 10°; no  
reflection region with a complex  
background shape

Profile function: pseudo-Voigt  
Weighting scheme based on  
measured s.u.'s  
( $\Delta/\sigma$ )<sub>max</sub> = 0.01

**Tl<sub>2</sub>BeF<sub>4</sub> at 300 K**

## Crystal data

$a = 7.7238$  (2) Å  
 $b = 5.90226$  (17) Å  
 $c = 10.4499$  (3) Å

$V = 476.39$  (2) Å<sup>3</sup>  
 $D_x = 6.884$  Mg m<sup>-3</sup>  
 $T = 300$  K

## Data collection

$2\theta_{\text{min}} = 6.3$ ,  $2\theta_{\text{max}} = 125.5^\circ$

## Refinement

$R_p = 0.036$   
 $R_{\text{wp}} = 0.048$   
 $R_{\text{exp}} = 0.076$   
 $R_B = 0.075$

$S = 0.63$   
934 reflections  
35 parameters

**Tl<sub>2</sub>BeF<sub>4</sub> at 200 K**

## Crystal data

$a = 7.69999$  (15) Å  
 $b = 5.86734$  (11) Å  
 $c = 10.4039$  (2) Å

$V = 470.03$  (2) Å<sup>3</sup>  
 $D_x = 6.977$  Mg m<sup>-3</sup>  
 $T = 200$  K

## Data collection

$2\theta_{\text{min}} = 6.3$ ,  $2\theta_{\text{max}} = 125.5^\circ$

## Refinement

$R_p = 0.042$   
 $R_{\text{wp}} = 0.055$   
 $R_{\text{exp}} = 0.076$   
 $R_B = 0.072$

$S = 0.73$   
924 reflections  
35 parameters

**Tl<sub>2</sub>BeF<sub>4</sub> at 150 K**

## Crystal data

$a = 7.69020$  (13) Å  
 $b = 5.84889$  (9) Å  
 $c = 10.37848$  (17) Å

$V = 466.82$  (1) Å<sup>3</sup>  
 $D_x = 7.025$  Mg m<sup>-3</sup>  
 $T = 150$  K

## Data collection

$2\theta_{\text{min}} = 6.3$ ,  $2\theta_{\text{max}} = 125.5^\circ$

## Refinement

$R_p = 0.047$   
 $R_{\text{wp}} = 0.063$   
 $R_{\text{exp}} = 0.076$   
 $R_B = 0.075$

$S = 0.83$   
918 reflections  
35 parameters

**Table 1**

Average Be–F and Tl–F distances (Å) and F–Be–F angles (°) for Tl<sub>2</sub>BeF<sub>4</sub> at each temperature.

Temperature (K)	Be–F	Tl–F	F–Be–F
300	1.534 (8)	3.040 (8)	109.5 (3)
200	1.537 (6)	3.022 (6)	109.47 (20)
150	1.539 (5)	3.014 (5)	109.47 (18)
100	1.546 (4)	3.004 (4)	109.47 (14)
50	1.548 (4)	2.997 (5)	109.46 (13)
1.5	1.560 (4)	2.996 (5)	109.46 (14)

**Tl<sub>2</sub>BeF<sub>4</sub> at 100 K**

## Crystal data

$a = 7.68265$  (11) Å  
 $b = 5.83059$  (8) Å  
 $c = 10.35278$  (15) Å

$V = 463.75$  (1) Å<sup>3</sup>  
 $D_x = 7.072$  Mg m<sup>-3</sup>  
 $T = 100$  K

## Data collection

$2\theta_{\text{min}} = 6.3$ ,  $2\theta_{\text{max}} = 125.5^\circ$

## Refinement

$R_p = 0.048$   
 $R_{\text{wp}} = 0.062$   
 $R_{\text{exp}} = 0.076$   
 $R_B = 0.063$

$S = 0.82$   
913 reflections  
35 parameters  
( $\Delta/\sigma$ )<sub>max</sub> = 0.01

**Tl<sub>2</sub>BeF<sub>4</sub> at 50 K**

## Crystal data

$a = 7.67874$  (9) Å  
 $b = 5.81248$  (7) Å  
 $c = 10.32788$  (12) Å

$V = 460.96$  (1) Å<sup>3</sup>  
 $D_x = 7.115$  Mg m<sup>-3</sup>  
 $T = 50$  K

## Data collection

$2\theta_{\text{min}} = 6.3$ ,  $2\theta_{\text{max}} = 125.5^\circ$

## Refinement

$R_p = 0.053$   
 $R_{\text{wp}} = 0.068$   
 $R_{\text{exp}} = 0.076$   
 $R_B = 0.061$

$S = 0.90$   
905 reflections  
35 parameters

**Tl<sub>2</sub>BeF<sub>4</sub> at 1.5 K**

## Crystal data

$a = 7.67735$  (10) Å  
 $b = 5.80377$  (8) Å  
 $c = 10.31316$  (13) Å

$V = 459.53$  (1) Å<sup>3</sup>  
 $D_x = 7.137$  Mg m<sup>-3</sup>  
 $T = 1.5$  K

## Data collection

$2\theta_{\text{min}} = 7.3$ ,  $2\theta_{\text{max}} = 125.5^\circ$

## Refinement

$R_p = 0.067$   
 $R_{\text{wp}} = 0.085$   
 $R_{\text{exp}} = 0.093$   
 $R_B = 0.069$

$S = 0.91$   
901 reflections  
35 parameters

Rietveld refinement of the six powder diffraction patterns was carried out with the program *FULLPROF* (Rodríguez-Carvajal, 2005) and visualization of the results was performed using the program *WINPLOTR* (Roisnel & Rodríguez-Carvajal, 2005). The experimental profiles were all modelled using a pseudo-Voigt profile shape function, with five adjustable parameters ( $U$ ,  $V$ ,  $W$ ,  $\eta$  and  $X$ ); initial values were obtained from the instrumental resolution parameters. After preliminary refinements to establish the scale factor, zero-point displacement, cell parameters and profile parameters, several cycles were performed to refine the atomic positions and isotropic displacement parameters. The starting values for the atomic positions were those of the  $\beta$ -K<sub>2</sub>SO<sub>4</sub> structure, in space group *Pnma*. Space group *Pn2<sub>1</sub>a* was also examined, without any improvement. Owing to the poor values obtained for the agreement factors and the modulated residuals that remained after the refinements, it was necessary to apply a Fourier filtering treatment in order to model the background and to improve the results. This can be justified because from the modulated residues it has been possible to calculate the

radial distribution function of other fluoroberyllates, because of the co-existence of an amorphous phase with the crystalline material (da Silva *et al.*, 2005).

For all temperature determinations, cell refinement: *FULLPROF* (Rodríguez-Carvajal, 2005); program(s) used to refine structure: *FULLPROF*; molecular graphics: *DIAMOND* (Brandenburg & Berndt, 1999); software used to prepare material for publication: *FULLPROF*.

---

Supplementary data for this paper are available from the IUCr electronic archives (Reference: FA1150). Services for accessing these data are described at the back of the journal.

---

## References

- Aiki, K. & Hukuda, K. (1969). *J. Phys. Soc. Jpn*, **26**, 1066–1076.
- Arend, H., Muralt, P., Plesko, S. & Altermatt, D. (1980). *Ferroelectrics*, **24**, 297–303.
- Brandenburg, K. & Berndt, M. (1999). *DIAMOND*. Crystal Impact GbR, Bonn, Germany.
- Brown, I. D. (1992). *Acta Cryst.* **B48**, 553–572.
- Fábry, J. & Brezewski, T. (1993). *Acta Cryst.* **C49**, 1724–1727.
- Fábry, J. & Pérez-Mato, J. M. (1994). *Phase Transitions*, **49**, 193–229.
- Friese, K., Goeta, A. E., Leech, M. A., Howard, J. A. K., Madariaga, G., Pérez-Mato, J. M. & Brezewski, T. (2004). *J. Solid State Chem.* **177**, 1127–1136.
- González-Silgo, C., Solans, X., Ruiz-Pérez, C., Martínez Sarrión, M. L., Mestres, L. & Bocanegra, E. (1997). *J. Phys. Condens. Matter*, **9**, 2657–2669.
- Hoshino, S., Vedam, K., Okaya, Y. & Pepinsky, R. (1958). *Phys. Rev.* **112**, 405–411.
- Rodríguez-Carvajal, J. (2005). *FULLPROF*. Version 3.20. Laboratoire Léon Brillouin (CEA-CNRS), France.
- Roisnel, T. & Rodríguez-Carvajal, J. (2005). *WINPLOTR*. Version of April 2005. Laboratoire Léon Brillouin (CEA-CNRS), France.
- Schlemper, E. O. & Hamilton, W. C. (1966). *J. Chem. Phys.* **44**, 4498–4509.
- Silva, I. da, González-Silgo, C., González-Platas, J., Rodríguez-Carvajal, J., Martínez-Sarrión, M. L. & Mestres, L. (2005). *J. Solid State Chem.* **178**, 1601–1608.
- Solans, X., Ruiz-Pérez, C., González-Silgo, C., Mestres, L., Martínez-Sarrión, M. L. & Bocanegra, E. (1998). *J. Phys. Condens. Matter*, **10**, 5245–5253.
- Srivastava, R. C., Klooster, W. T. & Koetzle, T. F. (1999). *Acta Cryst.* **B55**, 17–23.
- Yamada, N., Ono, Y. & Ikeda, T. (1984). *J. Phys. Soc. Jpn*, **53**, 2565–2574.